Research Article

Tahira Sultana, Khafsa Malik, Naveed Iqbal Raja, Sohail, Asma Hameed, Amir Ali*, Zia-ur-Rehman Mashwani, Muhammad Yousuf Jat Baloch*, and Abdulwahed Fahad Alrefaei

Phytofabrication, characterization, and evaluation of novel bioinspired selenium-iron (Se-Fe) nanocomposites using *Allium sativum* extract for bio-potential applications

https://doi.org/10.1515/gps-2023-0049 received March 19, 2023; accepted September 4, 2023

Abstract: Green nano-chemistry is an advanced research route covering eco-friendly fabrication approaches for synthesizing bimetallic nanocomposites (NCs) to enhance their therapeutic properties. The current study aims to phytofabrication, characterization, and bio-potential evaluation of novel selenium-iron (Se-Fe) NCs by utilizing garlic extract. The morphological and physicochemical features of Se-Fe NCs were evaluated by UV-visible spectroscopy, scanning electron microscopy, energy-dispersive X-ray, Fourier transform infrared, X-ray diffraction, and Zeta potential analysis. The findings showed that garlic cloves extract was a promising capping and reducing agent for the formulation of the NC. To explore the antioxidant potential of a bioinspired Se-Fe NC, 2,2-diphenyl-1-picrylhydrazyl and reducing power assays were performed. Furthermore, antioxidant efficacy was confirmed through antimicrobial activities against clinical pathogens. Phytosynthesized Se-Fe NCs (25, 50, 75, and 100 ppm) showed a dose-dependent response. Higher concentrations of Se-Fe NCs impose a more potent antioxidant and antimicrobial potential. The astonishing findings suggest that phytochemicals

in *Allium sativum* extract are useful reducing agents in the formulation of well-defined Se–Fe NCs, and such NCs could act as competitive inhibitors against pathogens. To the extent of our understanding, Se–Fe NC is the first time synthesized and demonstrates the distinctiveness of green chemistry and will give multifunctional applications in nano-biotechnology.

Keywords: Green chemistry, Se–Fe nanocomposites, synthesis and structural characterization, antioxidant potential, antimicrobial activity

1 Introduction

Nanoscale materials are entities with a size of 1-100 nm, according to the definition given in the context of chemistry. In recent decades, these nanomaterials have contributed significantly to the exponential growth of nanoscience, green chemistry, and nano-biotechnology [1]. However, nanomaterials frequently deviate considerably from their macroscale counterparts regarding their biological, physical, and chemical characteristics despite possessing similar chemical compositions [2]. A new addition to the line of nanotechnology is the formulation of nanocomposites (NCs). An attempt to investigate the uniqueness of a single nanocomponent can be overloaded by adding multiple other nanocomponents that deliver a lot of practical synergistic potential in various biomedical fields [3]. Monometallic nanomaterial properties can be enhanced by combining the other material, resulting in the formation of hybrid NCs [4]. According to some reports, these are the materials of the twenty-first century because they possess special architectural features and character combinations that are not present in traditional composites. Therefore, bimetallic NCs are enormously essential and have gained special attention among scientists in the medicinal chemistry and biomedical area to treat many diseases [5] effectively. There is still much to learn about these characteristics in

Tahira Sultana, Khafsa Malik, Naveed Iqbal Raja, Asma Hameed, Zia-ur-Rehman Mashwani: Department of Botany, PMAS Arid Agriculture University, Rawalpindi, Punjab 46300, Pakistan Sohail: College of Biosciences and Biotechnology, Yangzhou University, Yangzhou 225009, Jiangsu, China

Abdulwahed Fahad Alrefaei: Department of Zoology, College of Science, King Saud University, P.O. Box 2455, Riyadh 11451, Saudi Arabia

^{*} Corresponding author: Amir Ali, Department of Botany, PMAS Arid Agriculture University, Rawalpindi, Punjab 46300, Pakistan, e-mail: amirkhan31530@gmail.com

^{*} Corresponding author: Muhammad Yousuf Jat Baloch, College of New Energy and Environment, Jilin University, Changchun, 130021, China, e-mail: engr.yousuf@yahoo.com

general [6], despite the fact that their first indication was recorded in 1992 [7]. Generally, different approaches have been recognized for the fabrication of metal nanoparticles (NPs), such as chemical reduction [8], electrochemical [9], irradiation [10], thermal evaporation, as well as mechanical approaches and the green phytochemistry synthetic route [11]. Recently, numerous chemical and classical physical methods have been applied in NP synthesis but have gained a detrimental impact on biological and environmental concerns due to the high energy utilization and use of excessive toxic chemicals [12,13]. In order to solve these demonstrated environmental issues, exceptional attention has been focused on developing environmentally benevolent green nanomaterials that are free from toxic chemicals, more stable, and cost-effective in their fabrication [14–16]. Consequently, there is growing enthusiasm and demand for efficient green nanochemistry [17,18] because of the enormous strides it has made to represent one of the top explored and prospering fields because of its applicability in diverse human well-being fields [19]. When nanomaterials are adequately prepared by green synthetic procedures, they show remarkable unique emerging properties and astonishing applications compared to their bulk materials [20-22]. The most extensively used approach for synthesizing biocompatible NPs is the fabrication of NPs through plant extracts. This widely explored method has a significant benefit in that plants are abundant, simple to get, considerably safer to handle, and act as a reservoir of several phytomolecules or secondary metabolites that act as potent biocatalysts [23,24]. Garlic is a well-known herb, known from ancient times as Allium sativum, which is the second-largest growing crop worldwide. The major account of natural bioactive constituents in garlic extract is organosulfur-based array of phytochemical compounds with a wide range of biological and modulated therapeutic potential and are targeted for the biogenic formulation and synthesize stable nanomaterials [25]. The extract of these cloves contains an array of phytochemical compounds that can act as reducing agents. Garlic-based NPs were mainly exploited in the therapeutics fields and, to a lesser extent, in agriculture, food, and related areas [26].

The literature review revealed that various monometallic and their oxide NPs are formulated by biological means effectively. Still, bioinspired hybrid, bi, or tri-metallic NCs are reported significantly less. Selenium and iron monometallic NPs fabricated by phytochemical-based approaches have gained much interest with increasing green chemistry enthusiasm because of their fascinating application in biochemistry, environmental remediation, biomedical fields such as drug delivery systems, pharmaceutical, food industries, antimicrobial, anticancer, antioxidants, neurodegenerative

disease and also in the agricultural domain owing to nontoxicity as both are essential nutrients [27–29]. Iron NPs have immense application in the biomedical field due to their super-magnetic potential and excellent antimicrobial and antioxidant properties [30]. In one of the documented studies, Allium saralicum extract-assisted iron NPs showed significant antifungal, antibacterial, antioxidant, and wound healing potential. Remarkable results reported that Fe NPs inhibited the growth of all fungi and bacteria dose dependently and significantly showed antioxidant activity [31]. In another study, it is reported that Eucalyptus robusta extractmediated iron NPs showed a remarkable antioxidant effect. this attribute making FeNPs potent candidate for many pharmacological applications where free radicals play a decisive role [32]. Similarly, selenium NPs have been introduced as a trace mineral in biomedical that is considered an alternative therapy for cellular damage and possesses antimicrobial and anticancer potential [33,34]. Many reported studies revealed that the green formulation of selenium NPs exhibited promising antimicrobial functionality against the Gram-positive and Gram-negative bacteria [35,36]. Previous in vivo and in vitro studies have shown that green-fabricated selenium NPs are potent antimicrobial agents at the nanoscale that suppress the growth of multicellular and unicellular fungi up to 70% [6,37]. Selenium is the primary constituent of antioxidant selenoproteins. Moreover, several in vitro antioxidant surveys highlight that plant-mediated Se NPs have remarkable antioxidant activity that confers the resistance against oxidative stress by scavenging of free radicals [38,39]. The mechanism behind antimicrobial behavior is that they react with thiol protein, which disrupts the membrane permeability and stability, and leads to the leakage of membranes. After internalization, these NPs damage the cellular organelles, and macromolecules ultimately cause cell death [40,41]. Because of the broad range of applications of selenium and iron NPs, the present study was devoted to fabricating NCs using phytoconstituents as reducing agents for getting synergistic modulated potential. Due to their high bioavailability, it is the first and foremost attempt for the synthesis of selenium-iron (Se-Fe) composites by bioreduction of sodium selenite and iron sulfate salts using A. sativum bud extract with synergistic characters which have never been achieved by other conventional methods. The garlic extract-mediated NCs were well characterized through various analytical techniques such as UV-visible spectrum was used to ensure the composite formation, morphology, and surface topography by scanning electron microscope (SEM), and stretching vibrations or functional groups were detected via Fourier transform infrared (FTIR) techniques. Energydispersive X-ray (EDX) spectroscopy was done to know the elemental composition present in prepared Se-Fe NCs.

The novelty of our research study is based on the fact that there has yet to be any work reported on phytofabrication and application of Se-Fe NC. Moreover, the newly synthesized material was assessed for biopotential applications such as antioxidant and antimicrobial activities.

2 Materials and methods

The phytofabrication of Se-Fe NCs was carried out in the Nano-biotechnology Laboratory at the Department of Botany, PMAS Arid Agriculture University Rawalpindi. Furthermore, bioinspired Se-Fe NCs were evaluated for their bio-potential applications.

2.1 Materials

All reagents that were used in the current study are of analytical grade for accurate results. Hydrated salts used for NCs syntheses like sodium selenite and iron sulfate and chemicals for antimicrobial study such as 2,2-diphenyl-1picrylhydrazyl (DPPH), ascorbic acid, Mueller-Hinton nutrient agar media, potato dextrose agar (PDA), and methanol were purchased from Sigma-Aldrich. The deionized water was used throughout the whole study. All glasswares were properly washed and autoclaved. Garlic clove extract, selenium, and iron salt solutions were prepared in distilled water. The biological reduction of selenium and iron salt solutions for synthesizing its NCs was made by garlic extract. Agar well diffusion assay was used for the antimicrobial experiment.

2.2 Preparation of A. sativum plant extract

The preparation of garlic extract was initiated after the collection of garlic buds (shown in Figure 1) and peeled off the buds, then washed thoroughly with deionized water to remove all the dust and impurities. After drying the plant material, 20 g of fresh buds were crushed into a thick paste. The obtained content is boiled in 400 mL distilled water on a hot plate for 15 min and then cooled down at room temperature. The resulting extract was ultimately filtered through Whatman filter paper for the pure agueous plant extract. The final extract was used to reduce the selenium and iron salts into NCs [42].

2.3 Phytosynthesis of Se-Fe NC

To synthesize Se-Fe NCs, 5 mM aqueous salt solutions of sodium selenite and iron sulfate are freshly prepared by dissolving salts in distilled water. In total, 5 mM selenium and 5 mM iron salt solutions are mixed equally in the flask and kept on a magnetic stirrer to form a homogenous Se-Fe salt solution. About 100 mL of the prepared garlic bud extract was added continuously in aqueous salt solutions dropwise. This reaction mixture was continuously heated at 70°C and stirred until the color of the solution changed from clear salt solutions to light brown to dark brown, which represents the first indicative characteristic of Se-Fe NCs (as shown in Figure 2). Se-Fe NCs were visually confirmed by the sequential color change of the reaction mixture from transparent to light brown to

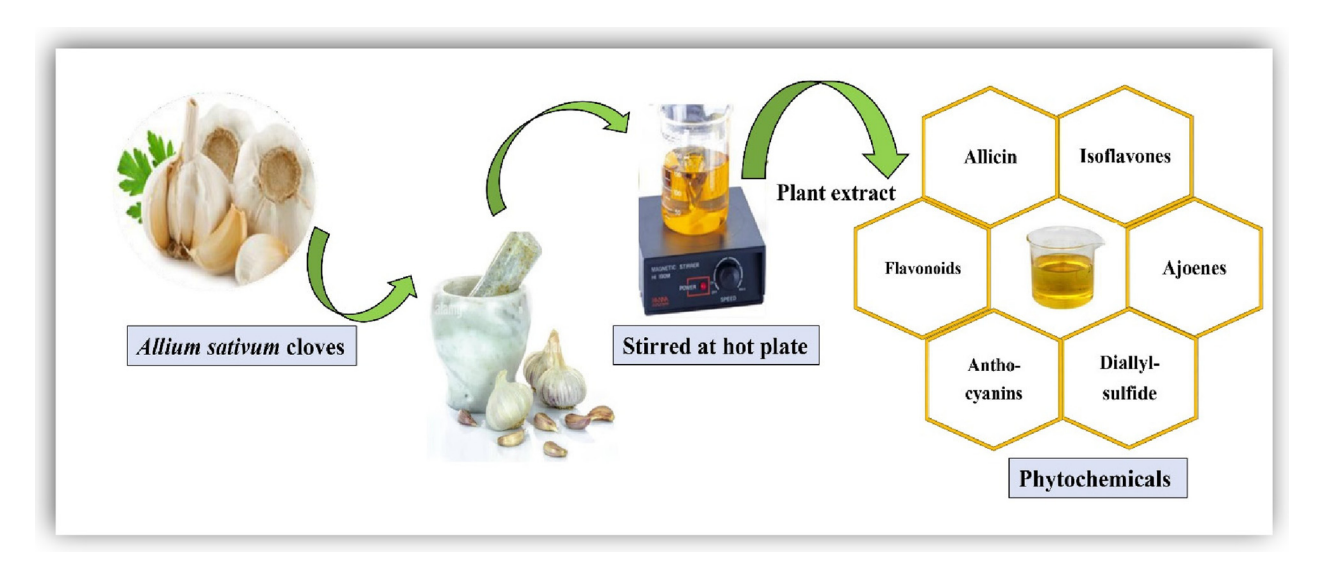


Figure 1: Schematic presentation of A. sativum plant extract.

4 — Tahira Sultana et al. DE GRUYTER

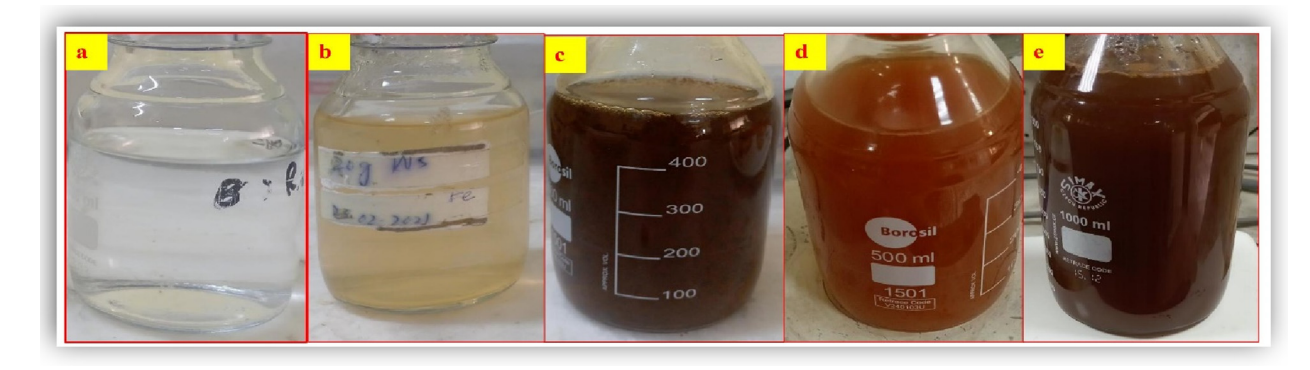


Figure 2: Visual observation of phytosynthesized Se–Fe NC solution: (a) selenium salt solution, (b) iron salt solution, (c) Se–iron salt solutions, (d) and (e); Se–Fe NCs solutions at different stirring times and increasing concentration of reducing agent (garlic extract).

brackish to dark brown, which indicates the reduction reaction. Selenium and iron from their respective salt solutions transformed into Se–Fe NCs at the required concentration of garlic extract. The minimum and optimal concentrations of garlic extract have an immense role in the reaction process. The obtained NC solution was centrifuged at 10,000 rpm for about 10 min to separate the NCs from impurities. The obtained NCs were rinsed in distilled water, resuspended in methanol, and centrifuged thrice. After complete purification, the pellet was collected and dried for 12 h in a drying oven at 400°C to obtain Se–Fe NC in powder form for further characterization, including, optical, morphological, and chemical characterization of the NC. The freshly phytosynthesized Se–Fe NCs were studied through various characterization techniques.

2.4 Structural characterizations of bioinspired Se-Fe NCs

2.4.1 UV-visible spectroscopy

The original formulation and optical characteristics of Se–Fe NCs were assessed using UV–visible spectrophotometry (Labomed UVD 3500, Los Angeles, CA, USA), which recorded absorbance from 200 to 900 nm.

2.4.2 FTIR spectroscopy

All transformations in the synthesis process were specifically analyzed through an FTIR spectrometer (Perkin-Elmer FTIR-Spectrum, Akron, Ohio, USA) to ensure the biomolecules naturally occurring in garlic extract, which plays a role in metal reduction, stability, and creation of Se–Fe NCs. The dried NC

was homogenized with potassium bromide, and FTIR analysis from 400 to 4,000 cm⁻¹ spectral range [43] was carried out.

2.4.3 SEM analysis

The topography or surface morphology of green synthesized Se–Fe NCs was determined through SEM (SIGMA) analysis. The SEM worked at 5 kV and at ×10k magnification. For the sample preparation, a drop coating method was adopted in which the sample was put on a copper grid that was coated by carbon. For drying, the resulting prepared sample was placed under the mercury lamp for 5 min. The extra solution was wiped off by blotting paper. The surface micrographs of the Se–Fe NC were observed at different magnifications [44].

2.4.4 EDX spectroscopy

The elemental analysis of bioinspired Se–Fe NCs was carried out by the EDX instrument (SIGMA). Thin carbon films were used for the sample preparation.

2.4.5 X-ray diffraction (XRD) characterization

Amorphous or crystalline state of the Se–Fe NCs was analyzed via XRD spectroscopy. The dried sample of Se–Fe NCs was loaded on XRD spectroscopy (Shimadzu XRD-6000) in $20-80^{\circ}$ range at a 2θ angle.

2.4.6 Zeta potential analysis

Zeta potential analysis was performed to determine the charge distribution on the Se-Fe NC surface using the

Zetasizer Nano Series (Malvern). For sample preparation, Se-Fe NCs were added in distilled water, and then the sample sonicated for 8 min. After sonication, about 0.5 mL of NC suspension was placed in a cuvette for determination of the electric charge distribution of the particles.

2.5 Antioxidant activity of bioinspired Se-Fe NCs

Free radical scavenging activity of novel green synthesized Se-Fe NCs was determined through the DPPH method. The DPPH stock solution of 1 mM concentration was prepared in methanol. Then, newly synthesized Se-Fe NC solutions were composed of various concentrations (25, 50, 75, and 100 ppm) and added to the DPPH solution separately. The resulting prepared solutions were finally incubated in the dark for about 30 min, and then the absorbance of blank (methanol), ascorbic acid (standard), and a sample was calculated through a UV-visible spectrometer (BioAquarius CE 7250, Cambridge, UK) at the 517 nm wavelength. The percentage of DPPH inhibition or free radical scavenging activity of Se-Fe NCs was calculated using the following formula [45]:

% DPPH inhibition = Absorbance (control)

- Absorbance (test)/Absorbance (control) \times 100

2.5.1 Reducing power assay

The reducing power of garlic extract-mediated Se-Fe NCs was analyzed by following the mentioned protocol [46]. In brief, various concentrations (25, 50, 75, and 100 ppm) of Se-Fe NCs were prepared and homogenized with 2.5 mL of phosphate buffer and 2.5 mL of 1% potassium ferricyanide. The resulting mixture was incubated for about 20 min at 500 °C and then cooled instantly. Subsequently, about 2.5 mL of 10% trichloroacetic acid was added to the above-mentioned resulting solution, which was then centrifuged at 3,000 rpm for 8 min. After that, equal amount (2.5 mL) of the supernatant layer was taken and mixed with distilled water. In the last step, 1 mL of 0.1% ferric chloride was added to the supernatant solution, and absorbance at 700 nm was measured using a spectrophotometer wavelength. In the experiment, ascorbic acid was taken as the standard. Reducing power percentage was noted by the following formula:

Reducing power (%) = (Blank absorbance

- Sample absorbance/Blank absorbance) × 100

2.6 Antimicrobial applications of phytogenic Se-Fe NCs

2.6.1 Micro-organism strains

In the current study, for antimicrobial activity, several bacterial and fungal strains were cultured on media plates containing nutrient agar and PDA, respectively. Both media were autoclaved (HVE-50 HIRAYAMA) at 121 for 15 min. The antimicrobial activity of the Se-Fe NC was evaluated against tested bacteria Escherichia coli (Gram-negative), Staphylococcus aureus (Gram-positive), and fungal strains (Aspergillus flavus, F. oxysporum) using antimicrobial assays, which are defined by their ability to portray the antimicrobial activity. The selected microorganism strains were obtained from the Department of Botany at PMAS Arid Agriculture University Rawalpindi.

2.7 Antibacterial and antifungal activity

Phytosynthesized Se-Fe NCs were tested for antimicrobial activity against clinical pathogen strains using the agar well diffusion method [47]. The selected pathogen strains were introduced on the Mueller-Hinton agar media and then spread on plates uniformly. A sterile metal cork borer was used to drill about 6 mm diameter wells in the agar plates. Different concentrations of Se-Fe NCs (25, 50, 75, and 100 ppm) were prepared, and 60 µL NC solutions were poured into specified wells. The antimicrobial efficacy of NCs was determined by measuring the inhibition zone diameter in millimeters around the designed wells with a measuring scale. In the case of antifungal activity, freshly cultured fungal spores were collected and placed on PDA. The spore count was adjusted to $2 \times 10^6 \, \text{CFU} \cdot \text{mL}^{-1}$ with the help of a hemocytometer. Antibiotics (Streptomycin, Terbinafine) were used as control. Petri dishes with bacterial culture were incubated in a dry oven at 37°C for 24 h and fungal plates at about 25°C for 72 h. The entire experiment was conducted in a highly sterilized environment.

2.8 Statistical analysis

All the experiments were conducted in a completely randomized design. Each treatment had three replicates that were repeated three times, and the data were analyzed statistically by using SPSS ver. 16.0 software (Chicago, IL, USA). The mean values and significant differences in the data were calculated using DMRT at p < 0.05.

3 Results and discussion

3.1 Visual observation of Se-Fe NCs

The present study revealed that the color of the reaction mixture for Se–Fe NCs was changed. When a reducing agent (garlic extract) was added, it transformed from transparent salt solutions to an ultimately dark brown composite product that was continuously stirred (Figure 2). This is the first indicator for the formation of NC solution. The respective metal ions were eventually reduced when they were exposed to garlic bud extract within 24 h of the incubation period. The previous studies also revealed that garlic extract was determined to be a promising reducing agent [48]. This color change due to the complete reduction of metal ions can be ascribed to the excitation of surface plasmon vibrations in the NP [49].

3.2 UV-visible spectra

The initial synthesis and optical properties of plant-mediated newly synthesized Se–Fe NCs were further confirmed by the UV–Vis spectrum. UV–visible analysis is considered to be an important method to ascertain the stability and formulation of metal NPs present in the aqueous solution. Figure 3 shows the existence of selenium nanostructures because of the excitation of plasmon longitudinal vibration at a broad plasmon surface resonance band 262 nm. Aside from that, the figure also illustrates the second absorbance peak at 296–316 nm, which implies the presence of iron NPs. These absorption peaks were confirmed by previous studies for the green synthesis of monometallic selenium and iron nanostructures. According to the literature, a spectrum of nanostructures at 262 nm [50], at 265 nm [51], and broad spectra recorded within

a wavelength of 200–500 nm display the presence of selenium NPs [52,53]. Jagathesan and Rajiv [54] stated that using UV–visible analysis revealed that *Eichhornia*-mediated FeNPs had a broad absorption spectrum at 379 nm. Throughout the whole spectral range, a wide absorbance band was found, particularly around 350 and 500 nm [55,56]. Respective wavelengths of selenium and iron are discrete and separated. The Se and Fe nanomaterials in a solution generally form aggregates and are discovered to be stable in suspension. SPR bands are often affected by the synthesized NPs' shape, size, surface topography, elemental composition, and electrostatic environment [57].

3.3 FTIR spectroscopy

An evaluation of the FTIR spectrum of garlic clove extract with the Se-Fe NC FTIR spectrum shows many sharp peaks, indicating that the phenolic compounds of garlic extract interact with selenium and iron metal ions. These phytochemicals of extract counter for reducing, stabilizing, and capping agents that are responsible for the formulation of stabilized Se-Fe NCs. The FTIR spectra, represented in Figure 4, exploit the maximum information that confirms the bonding nature of garlic extract-mediated Se-Fe NC on the basis of identifying a number of functional groups residing on the surface of nanostructures. In order to confirm the NC's structure, procedures from the literature were applied to identify the conspicuous peaks. The spectrum displays a number of prominent peaks at certain regions that are clearly distinguished from weak bands. From the spectrum, the most substantial peak was observed at 3,434 cm⁻¹, which corresponds to (OH) the functionality of the hydroxyl group excessively found in phenolic compounds, which plays a crucial role in the stable formulation of NCs [58].

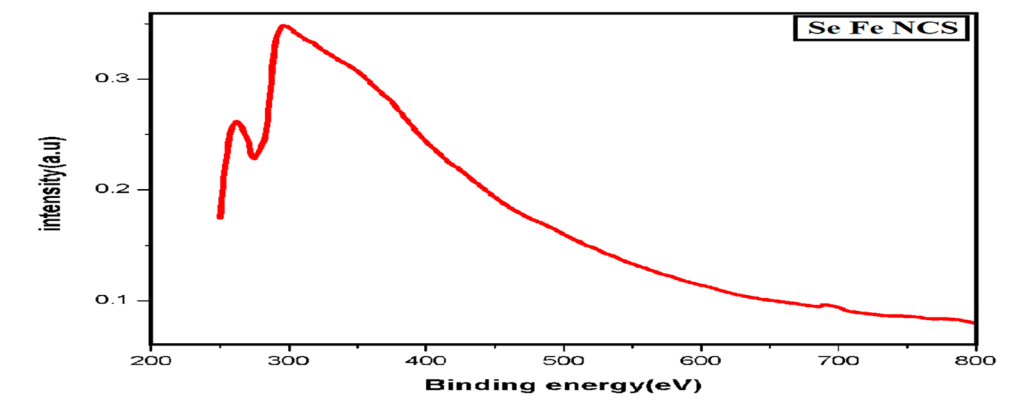


Figure 3: UV–Visible spectrum of Se–Fe NCs.

The range within 600 to 1,500 cm⁻¹ was regarded as a fingerprint zone and is indicative of the compound. The sharp peaks in this trademark region for Se-Fe NCs were 1,012 cm⁻¹ for C-N group stretching and also due to ether linkage. Moreover, the C-H distortion peak appeared at 1,375 cm⁻¹, respectively. The absorption peak at 1,426 cm⁻¹ in Se–Fe NC FTIR spectra represents the C=C stretch. The two absorption peaks observed at around 1,283 to 1,083 cm⁻¹ range were due to the overlapping of stretch bands of the alcoholic O-H as well as vibrations of C-O-C ether linkage [1]. In addition, as depicted in Figure 3, most of the significant and conspicuous peak noticed at 1.571 cm⁻¹ was ascribed to the bending frequencies of the amide group (N-O) NH. In addition, two weak peaks appear in spectra at 819 and 649 cm⁻¹ due to out-of-plane C-H bending and C-X stretching found in alkyl halides, respectively. Ultimately, the FTIR spectra showed all the potential peaks that demonstrate the NC formation. It also illuminated the significance of phytochemicals present in plant extract as capping or reducing agents in stabilizing the overall NC structure. The absorption or stretching peaks due to various functional groups residing on nanomaterials are confirmed through all the reported literature; bands at 3,471 and 1,682 cm⁻¹ elaborate stretching and bending vibrations of -OH. Furthermore, C-H stretching is linked to the sharp peaks that appeared at 2,359 and 1,483 cm⁻¹. Consequently, two vast peaks observed at 2,999 and 2,359 cm⁻¹ might be associated with O-H bending vibration. It was considered that water molecules adhered to the surface. The small peak at 1,132 cm⁻¹ is attributable to the stretching vibration of the C-OH bond [59]. One of the studies documented that O-H, N-H, C=O, and C-H functional groups interact with selenium atoms to form NPs [60]. Another

scientific study also conducted FTIR spectroscopy and verified that the presence of phenols and other alkenes in plant extract due to O–H, C–H and C–C stretching are involved in the formulation of iron NPs [61].

3.4 SEM analysis

The surface topography of newly phytosynthesized Se-Fe NCs was investigated through SEM analysis. It is regarded as one of the most renowned analytical approaches for demonstrating the size and topography of NCs [5]. Figure 5 demonstrates typical SEM photographs of garlic extractbased Se-Fe NCs, representing the uniform surface topography and spherical shape with a fine crystallite nature having a particle size in the 50-80 nm range. Previous literature confirmed SEM results of biosynthesized iron oxide monometallic nanomaterials in the 70 nm range [62] and selenium in the 45-90 nm range [63]. These images depict that plant-mediated nanomaterial was highly uniform distributed and in a stable conformation. Furthermore, these micrographs revealed no indication of conglomeration with an unequivocal distribution of the particles, confirming the stable nature of synthesized NPs.

3.5 EDS analysis

To determine the selenium and iron presence in the phytogenic synthesized Se–Fe nanomaterials, EDX spectroscopy

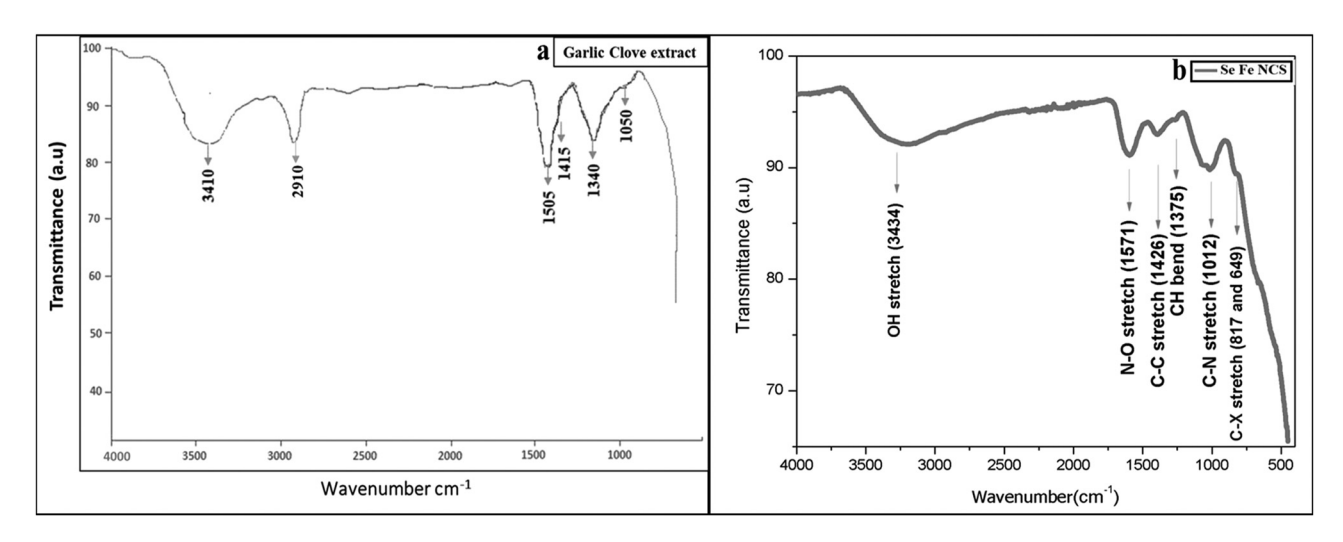


Figure 4: FTIR investigation of (a) garlic clove extract and (b) Se-Fe NCs.

8 — Tahira Sultana et al. DE GRUYTER

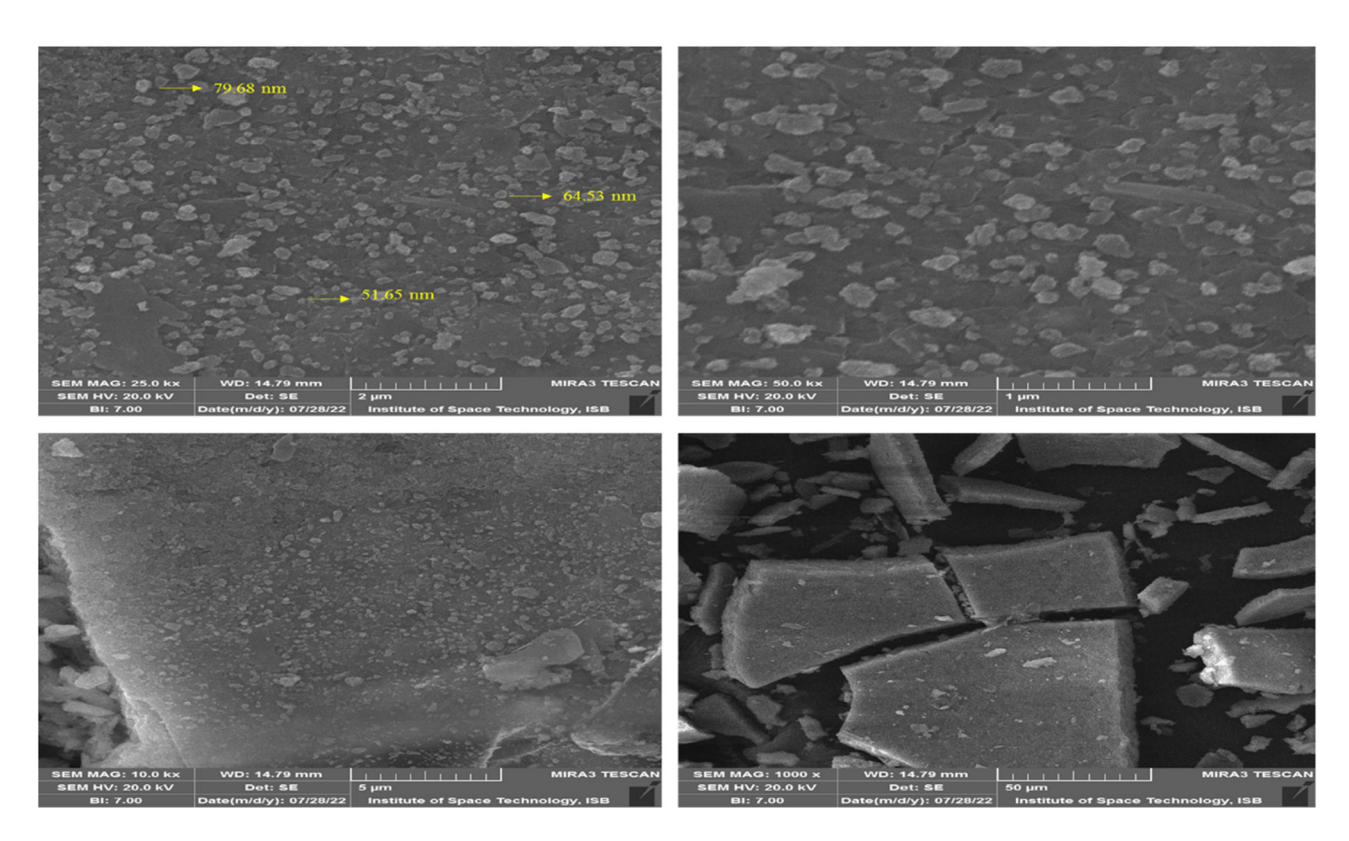
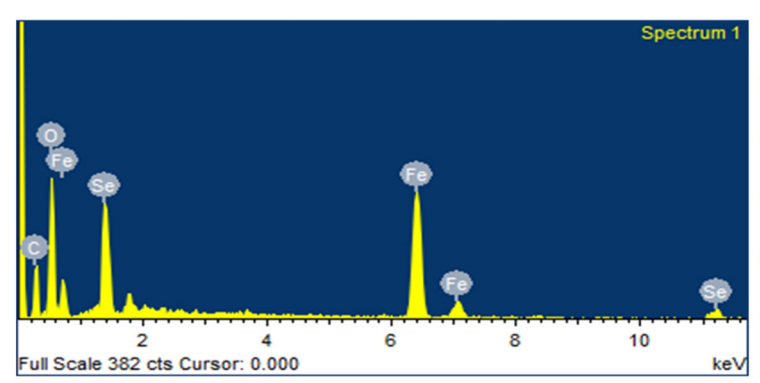


Figure 5: SEM images of Se-Fe NC at various magnifications.

technique was used. Figure 6 elucidates peaks comparable to oxygen, selenium, and iron elements. The resulting NC (Se–Fe) is pure because no residual impurities were noticed. The presence of Se, Fe, and O confirms the formation of Se–Fe NCs. According to recently reported literature, the NC formulation is readily explained by the indication for the oxygen atom that was also identified in Se–Fe NCs [5]. The proportion of all the existing elements in the Se–Fe nano-based composite is Fe (31.52%), O (30.08%), Se (15.11%), and C (23.28%) based on atomic% analysis.

3.6 XRD analysis

Figure 7 depicts the XRD pattern for the green synthesized Se–Fe NCs. The pattern represents the crystalline nature of synthesized NCs because of the presence of Bragg's reflections. Peaks were identified using selenium diffraction signals (220) and (311) and iron signals (422), (511), (533), (620), and (622). The pattern shows d-spacing values for both selenium (JCPDS card No. 06-362) and iron (JCPDS card no. 39-1346). The EDX analysis explained that the presence



Element	Weight%	Atomic%
CK	23.28	42.37
O K	30.08	41.10
Fe K	31.52	12.34
Se L	15.11	4.18
Totals	100.00	100.00

Figure 6: EDX analysis of Se-Fe NC.

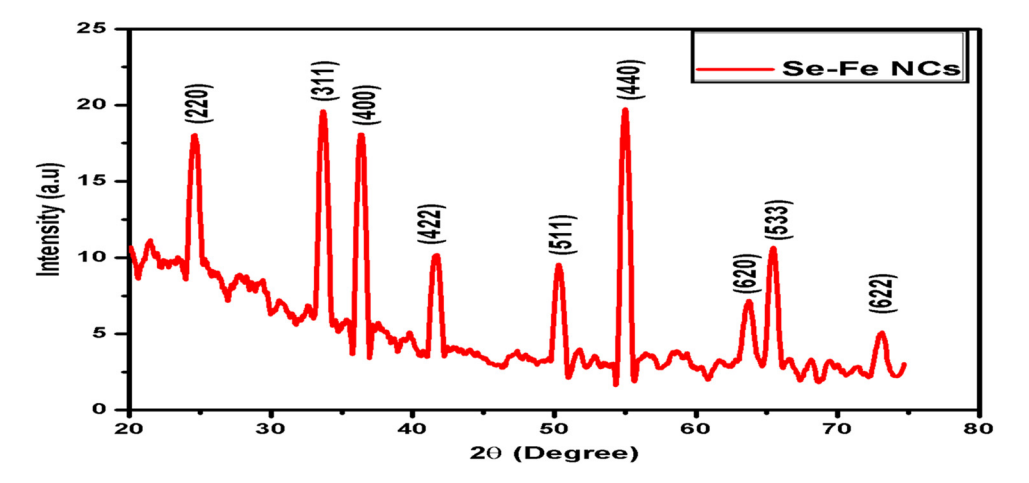


Figure 7: XRD analysis of Se-Fe NC.

of both selenium and iron peaks in a single pattern shows the formulation of Se–Fe NCs. Furthermore, the average crystallite size of Se–Fe NCs was estimated by Scherer's equation: $D=k\lambda/\beta\cos\theta$, where k is constant = 0.94, λ is the X-ray wavelength (0.15406 nm), β is the peak half width, and θ is the half of the Bragg's angle. By following the equation, the single crystal size of resulting NCs was predicted in the range of 14–20 nm. Moreover, narrow and sharp peaks in the spectrum illustrated that Se–Fe NCs have strong crystallinity.

3.7 Zeta potential spectroscopy

The zeta analysis is a useful characterization technique for knowing more about the stability of NPs. Zeta potential

distribution amplitude represents the nanomaterial's possible stabilization [64]. The zeta potential findings of the present study depicted the negative charge (-25.2 mV) on the Se-Fe NCs (Figure 8). In the suspension, if all the NPs have a positive or negative surface charge, then those particles will strongly repel to one another. There will be a minimum inclination for the NPs to join together, which represents their high stability [36]. The negative charge potential on formulated NCs probably leads to the strong stabilization of the Se-Fe NCs without aggregation. According to previous reports, the negative potential was found on green synthesized selenium (-24.4 mV) [34] and iron NPs (-16 mV) [62], respectively, and these stabilized nanomaterials do not turn to dark amorphous when they stored for a long time. The NPs with a higher zeta potential magnitude showed high stability because of stronger electrostatic repulsion among the NPs. Our results are aligned with the previous reported literature.

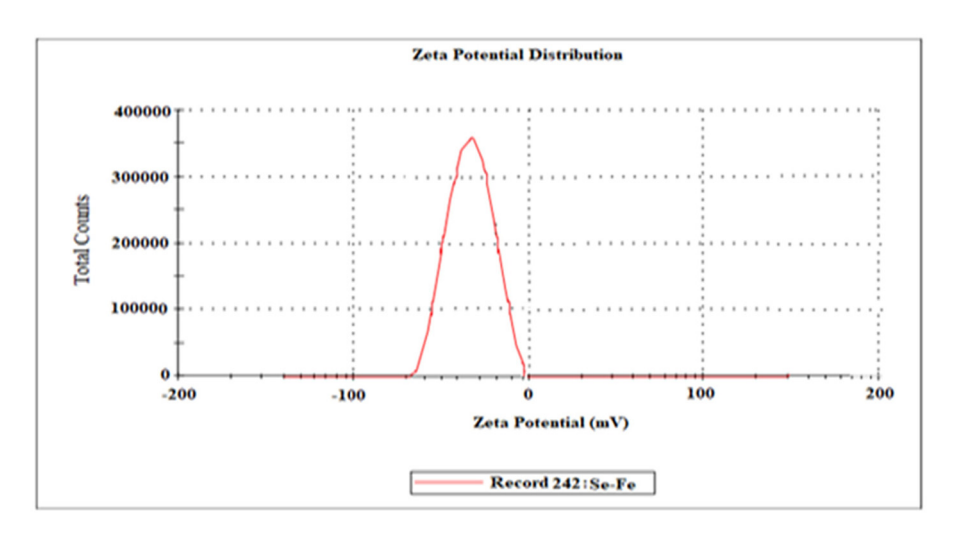


Figure 8: Zeta potential analysis of Se-Fe NC.

3.8 Bio-potential applications of biocompatible Se-Fe NCs

3.8.1 Antioxidant activity (DPPH)

One of the foremost promising and reliable methods for determining antioxidant effectiveness is the DPPH assay. which was designed using recognized and renowned practices. Owing to the accumulation of reactive oxygen species (ROS) in terms of free radicals, many types of persistent diseases, including oxidative damage, cancer, protein degradation, diabetes mellitus, and liver and brain dysfunctions, have emerged. In addition to this, the presence of ROS in the body is linked to a number of additional disorders, including aging, cataracts, and cardiovascular issues [65]. The DPPH efficacy of Se-Fe NCs was evaluated by observing a change in color. From Figure 9, it was observed that the DPPH scavenging method showed effective inhibition potential of Se-Fe NCs by increasing the concentration from 25 to 100 ppm. The maximum scavenging efficiency of biogenic Se-Fe NCs and standard (ascorbic acid) was 77.30% and 94.16%, respectively, at 100 ppm concentration. The potential of antioxidant activity of green synthesized nanomaterials was enhanced due to the influential association with various phytochemicals present in the bud extract of A. sativum, which are responsible for the synthesis of stable NCs. However, the protocol followed for the synthesis of Se-Fe nanomaterials tends to enhance the antioxidant potential and aid in the reduction of DPPH radicals. The plant extract phytochemicals adhered on nanomaterials are found to be electron-enriched species and neutralize the free radicals by donating electrons [66]. Current study outcomes were in line with the results of phytosynthesized iron and selenium NPs individually. Our results are strongly

coherent with previous studies in which the average percentage DPPH antioxidant efficacy of green synthesized selenium NPs was 75% inhibition at $600~\mu g \cdot m L^{-1}$ concentration [67]. Recently Kokila et al. [68] mentioned that plant-mediated 16 nm sized selenium NPs inhibit 50% scavenging potential at 22.5 $\mu g \cdot m L^{-1}$. Another study of biosynthesized iron NPs documented the DPPH scavenging activity 17.25% at 50 $\mu g \cdot m L^{-1}$. Iron NPs have a strong ability to donate an electron and serve as ROS scavengers or inhibitors; however, they act as primary antioxidants [69]. The DPPH scavenging activity assay outcomes in this current study show that plant-based NC was potently active.

3.8.2 Reducing power assay

Figure 9 depicts the reducing power of the garlic extractmediated Se-Fe dose-dependent NC response. By increasing the concentration of NCs and ascorbic acid (standard), reducing potential was increased consistently. The outcomes of the DPPH experiment revealed that Se-Fe NCs and ascorbic acid showed 76.17% and 87.52% scavenging activity through reducing assay, respectively. Surprisingly, Se-Fe NCs exhibited better results due to the excessive presence of an array of phytochemicals in the garlic extract. However, these secondary metabolites such as phenols, saponins, polyphenols, and sulfur-containing substances have antioxidant activity because these are electron donors [70]. Our study results are coherent with previous reports and observed that fenugreek seed-mediated iron NPs showed 60% reducing power at 110 μg·mL⁻¹ [71]. Due to their strong antioxidant potential, these iron NPs are potent aspirants for supplementary pharmacological studies where ROS production plays a critical role [32]. A recent study documented that garlic extract-

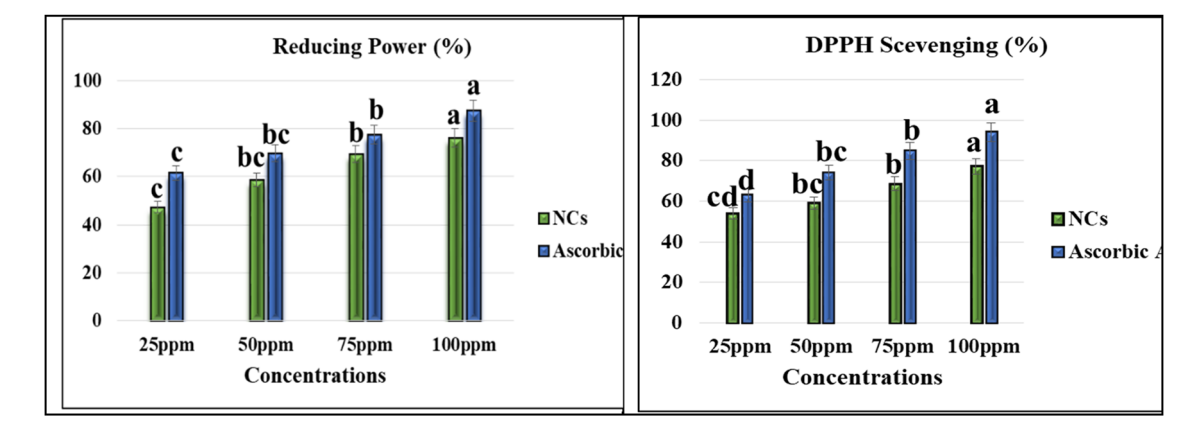


Figure 9: Antioxidant activities of Se–Fe NCs. Data represent the mean values of triplicates with \pm standard error for each treatment in three repeated experiments. Annotation of columns data with different alphabet (s) represents the significance at (p = 0.05).

Table 1: Zone of inhibition of biogenic Se–Fe NCs for selected clinical pathogens

Microbial strains	NC concentrations (ppm)			
	25 50 75 100 Zone of inhibition (mm)			
E. coli	13.88	18.1	23.09	26.89
S. aureus	15.06	19.89	24.96	29.04
A. flavus	10.11	13.26	17.96	22.66
F. oxysporum	13.11	16.74	21.1	24.32

based selenium NPs showed a maximum reducing power of 80.37% at 400 ppm concentration, which is a very high dose of NPs [72].

3.8.3 Antimicrobial activity of Se-Fe NCs

In the present work, the antimicrobial potential of phytosynthesized Se–Fe NC was checked and measured through the agar well diffusion method against selected clinical microbial strains, which were *E. coli, S. aureus, A. flavus,* and *Fusarium oxysporum.* Different concentrations of NCs ranging from 25, 50, 75, and 100 ppm were used and evaluated zone of inhibition against selected pathogens as presented in Table 1. The results represent that at 100 ppm concentration of NC zone of inhibition against *S. aureus*

is 29.04 mm, 26.89 for E. coli, 22.66 for A. flavus, and 24.32 for F. oxysporum. These outcomes documented better antimicrobial potential of garlic-mediated Se-Fe NCs than the garlic extract used as standard. At the same concentration (100 ppm) of A. sativum bud extract, several other inhibition zones, 26.38, 22.87, 18.11, and 19.93 mm, were observed, respectively. Outcomes of the study are confirmed with previous results in which iron NPs demonstrated that the maximum inhibition zone for Bacillus subtilis and Aspergillus niger was 19 mm [73], and Aloe vera-mediated selenium NPs showed inhibition zones 12 and 10 mm against S. aureus and E. coli, respectively [74]. In the current study, it was also observed that Gram-positive bacteria were shown to be more susceptible to Se-Fe NCs than Gramnegative. It could elucidate the sensitivity of bacteria to iron and selenium NPs because the thick peptidoglycan coating present on Gram-positive bacteria presumably allows for an adequate level of contact between pathogens and NPs. Comparatively, Gram-negative bacteria have a thin peptidoglycan coating in between their cytoplasmic and cell membranes, which serve as their boundaries. In this situation, getting Fe NPs into the thin layer is very challenging [75]. In reference to selenium NPs, they exhibit significant antagonistic effects on the membranes of Gram-negative bacteria and their polysaccharides. Due to this, bacterial fatality may require a more significant selenium nanomaterial accumulation on the surface of Gram-positive bacterial membranes. As a result, Gram-negative bacteria

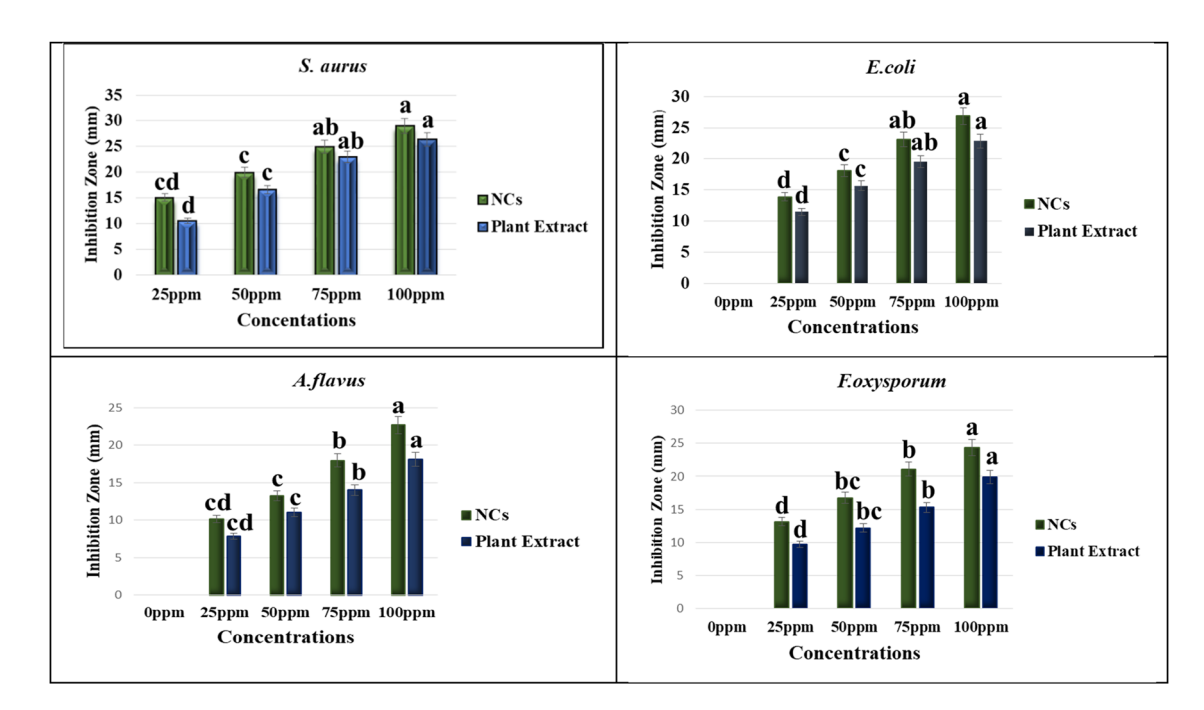


Figure 10: Antimicrobial activities of Se–Fe NCs. Data represent the mean values of triplicates with \pm standard error for each treatment in three repeated experiments. Annotation of columns data with different alphabet (s) represents the significance at p = 0.05.

12 — Tahira Sultana et al. DE GRUYTER

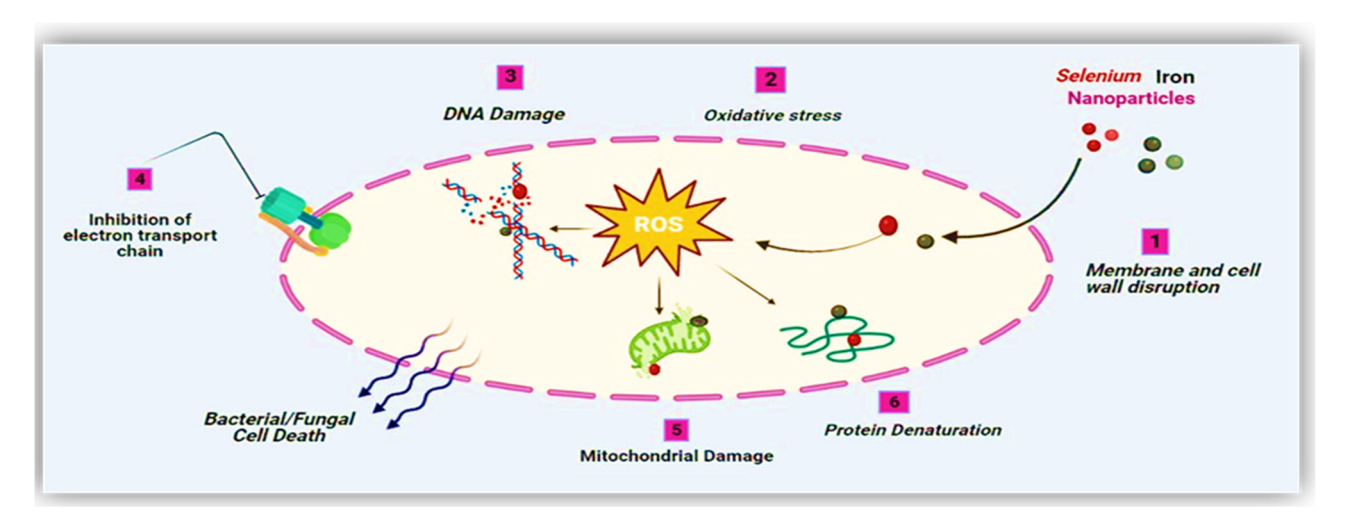


Figure 11: Antimicrobial mechanism of NPs.

show strong resistance power against SeNPs [76]. From the results mentioned above, it was considered that Se–Fe NCs are potent and promising antimicrobial nano-products in the treatment of pathogenic infections (Figure 10).

3.8.4 Antimicrobial mechanism of Se-Fe-based nanomaterials

In recent studies, different antimicrobial mechanisms of nanomaterials have been proposed. The antimicrobial action of NPs is generally defined as adhering to various models, such as NPs being causative agents for oxidative damage [77]. These release metal ions affect the antimicrobial potential of respective metal-based nanomaterials [78] and other non-oxidative approaches [79]. Eventually, these different mechanistic ways can happen concurrently. NPs inhibit the synthesis of the cell wall and cell's membranous system, disturb energy transduction pathways, free radicals such as ROS are produced, photocatalysis, interference with enzyme activity, and degrade DNA, amino acids, and proteins [80]. The results of the present work elucidate the mechanism of Se-Fe NCs, which disinfect the pathogens in several ways. Monometallic selenium NPs have garnered significant interest in treating clinically significant pathogens such as bacteria, fungi, viruses, and other parasites, due to their excellent therapeutic proficiency and nearly completely devoid of detrimental effects [81]. In another study, a leakage test was performed and demonstrated that many proteins and some polysaccharides were released out of the cells after reacting with green synthesized SeNPs. It was discovered that the rupture of cell walls and alterations in membrane permeability were responsible for the leakages of proteins and polysaccharides. Additionally, the

change in free radical concentration reveals that oxidative destruction may be a major factor in antimicrobial activities [82]. In contrast to the antimicrobial activity of iron monometallic NPs, the proposed mechanism is that particles accumulate in the cytoplasm and penetrate the cell wall of a pathogen in order to trigger the membrane to burst, resulting in the release of cellular substance and ultimately the death of the microorganisms [83]. The abovementioned outcomes from the current study clearly depict the synergistic potential of Se–Fe NCs in an antimicrobial mechanism that disrupts the cell membranes and causes oxidative stress (Figure 11).

4 Conclusion

This study successfully introduced green-synthesized Se-Fe NCs and their significant bio-potential applications for the first time, demonstrating the efficacy of green nano-chemistry in therapeutic applications. It is obvious from the results of the current investigation that A. sativum bud extract was proven to be an effective reducing agent, and it is an economically viable, efficient, and commercially feasible green synthesis method for the NC. The formation of Se-Fe NCs was confirmed through UV-Vis absorption spectra, which exhibit strong peaks in the range of 262–316 nm; surface morphology and particle size were identified from SEM, which showed that NCs were near to spherical shape and further crystallite size confirmed from XRD that was in 14-20 nm range. FTIR characterization confirmed the Se-O-Se and Fe-O-Fe types of bonding formation. Further elemental composition was investigated through the EDX spectrum, which confirmed the presence of Se, O, and Fe in the sample.

The stability of particles was assessed by zeta potential analysis, which showed that NCs are negatively charged. Synthesized NCs showed strong stability and antioxidant and antimicrobial efficacy due to the synergistic effect of selenium, iron NC, and phytochemicals adhered to the nanomaterials. Finally, the biogenic approaches enrooted the green revolution and an economic threat-less way for designing antimicrobial nano-products with required biocompatibilities. Future directions for our research will focus on the resulting NC specific characteristics and detailed applications.

Acknowledgements: We appreciate the Researchers Supporting Project (no. RSP2023R218), King Saud University, Riyadh, Saudi Arabia.

Funding information: We appreciate the Researchers Supporting Project (no. RSP2023R218), King Saud University, Riyadh, Saudi Arabia.

Author contributions: Khafsa Malik and Tahira Sultana: devised the study: Tahira Sultana: performed the experiments; Tahira Sultana: wrote the first draft; Khafsa Malik, Naveed Iqbal Raja: supervised the study; Zia-ur-Rehman Mashwani, Amir Ali, Asma Hameed, Sohail, Muhammad Yousuf Jat Baloch and Abdulwahed Fahad Alrefaei: edited, reviewed, and revised the manuscript. All authors reviewed and endorsed the final version of the manuscript for submission.

Conflict of interest: Authors state no conflict of interest.

Institutional review board statement: Not applicable.

Informed consent statement: Not applicable.

Data availability statement: The datasets generated during and/or analysed during the current study are available from the corresponding author on reasonable request.

References

- Ahmad MB, Tay MY, Shameli K, Hussein MZ, Lim JJ. Green synthesis and characterization of silver/chitosan/polyethylene glycol nanocomposites without any reducing agent. Int J Mol Sci. 2011:12(8):4872-84.
- Heidarpour F, Ghani WAWAK, Ahmadun FR, Sobri S, Zargar M, [2] Mozafari MR. Nano silver-coated polypropylene water filter: I. Manufacture by electron beam gun using a modified balzers 760 machine. Dig J Nanomater Biostruct. 2010;5:787-96.

- Panáček A, Kolář M, Večeřová R, Prucek R, Soukupová J, Kryštof V, et al. Antifungal activity of silver nanoparticles against Candida spp. Biomaterials. 2009;30(31):6333-40.
- [4] Sharma G, Kumar D, Kumar A, Ala'a H, Pathania D, Naushad M, et al. Revolution from monometallic to trimetallic nanoparticle composites, various synthesis methods and their applications: A review. Mater Sci Eng C. 2017;71:1216-30.
- Khan AU, Khan AU, Li B, Mahnashi MH, Alyami BA, Algahtani YS, [5] et al. Biosynthesis of silver capped magnesium oxide nanocomposite using Olea cuspidata leaf extract and their photocatalytic, antioxidant and antibacterial activity. Photodiagnosis Photodynamic Ther. 2021;33:102153.
- Schmidt D, Shah D, Giannelis EP. New advances in polymer/layered silicate nanocomposites. Curr OpSolid State Mater Sci. 2002;6(3):205-12.
- Gleiter H. Materials with ultrafine microstructures: retrospectives [7] and perspectives. Nanostruct Mater. 1992;1(1):1-19.
- Nikam AV, Prasad BLV, Kulkarni AA. Wet chemical synthesis of metal oxide nanoparticles: a review. CrystEngComm. 2018;20(35):5091-107.
- Starowicz M, Stypuła B, Banaś J. Electrochemical synthesis of silver [9] nanoparticles. Electrochem Commun. 2006;8(2):227-30.
- Jamkhande PG, Ghule NW, Bamer AH, Kalaskar MG. Metal nano-[10] particles synthesis: An overview on methods of preparation, advantages and disadvantages, and applications. J Drug Delivery Sci Technol. 2019;53:101174.
- [11] Garibo D, Borbón-Nuñez HA, de León JND, García Mendoza E, Estrada I, Toledano-Magaña Y, et al. Green synthesis of silver nanoparticles using Lysiloma acapulcensis exhibit high-antimicrobial activity. Sci Rep. 2020;10:12805.
- [12] Ahmad A, Wei Y, Syed F, Imran M, Khan ZUH, Tahir K, et al. Size dependent catalytic activities of green synthesized gold nanoparticles and electro-catalytic oxidation of catechol on gold nanoparticles modified electrode. RSC Adv. 2015;5(120):99364-77.
- [13] Ai J, Biazar E, Jafarpour M, Montazeri M, Majdi A, Aminifard S, et al. Nanotoxicology and nanoparticle safety in biomedical designs. Int J Nanomed. 2011;1117-27.
- [14] Shah M, Fawcett D, Sharma S, Tripathy SK, Poinern GEJ. Green synthesis of metallic nanoparticles via biological entities. Materials. 2015:8(11):7278-308.
- [15] Lagashetty A. Green synthesis and characterization of silver nanoparticles using piper betel leaf extract. Bull Adv Sci Res. 2015;1(5):136-8.
- [16] Amarendra DD. Biosynthesis of silver and gold nanoparticles using Chenopodium album leaf extracts. Colloids Surf A. 2010;369(3):27-33.
- Iravani S. Green synthesis of metal nanoparticles using plants. Green Chem. 2011;13:2638-50.
- Vaidyanathan R, Gopalram S, Kalishwaralal K, Deepak V, Pandian SR, Gurunathan S. Enhanced silver nanoparticle synthesis by optimization of nitrate reductase activity. Colloids Surf B Biointerfaces. 2010;75(1):335-41.
- Dikshit PK, Kumar J, Das AK, Sadhu S, Sharma S, Singh S, et al. Green synthesis of metallic nanoparticles: Applications and limitations. Catalysts. 2021;11(8):902.
- Hemanth NKS, Karthik KG, Bhaskara RKV. Extracellular biosynthesis [20] of silver nanoparticles using the filamentous fungus Penicillium sp. Arch Appl Sci Res. 2010;2(6):161-7.
- [21] Basavaraja S, Balaji SD, Lagashetty A, Rajasab S, Venkataraman A. Extracellular biosynthesis of silver nanoparticles using the fungus Fusarium semitectumm. Mater Res Bull. 2008;43(5):1164-70.

- [22] Ankamwar B, Ahmad DC, Sastry M. Biosynthesis of gold and silver nanoparticles using Emblica Officinalis fruit extract, their phase transfer and transmetallation in an organic solution. J Nanosci Nanotechnol. 2005;5(10):1665–71.
- [23] Parashar UK, Saxena PS, Srivastava A. Bioinspired synthesis of silver nanoparticles. Dig J Nanomater Biostruct. 2009;4:159–66.
- [24] Elumalai EK, Prasad TNVKV, Hemachandran J, Therasa SV,
 Thirumalai T, David E. Extracellular synthesis of silver nanoparticles
 using leaves of Euphorbia hirta and their antibacterial activities.
 J Pharm Sci Res. 2010;2(9):549–54.
- [25] Subbanna S, Gopenath TS, Basalingappa KM. Biogenic nanoparticles from *Allium sativum* and its bioactives applications. Eur J Mol Clin Med. 2020;7(08):212–32.
- [26] Krishna SBN. Emergent Roles of Garlic-Based Nanoparticles for Biomedical Applications-A Review. Curr Trends Biotechnol Pharm. 2021;15(3):349–60.
- [27] Johnson J, Shanmugam R, Lakshmi T. A review on plant-mediated selenium nanoparticles and its applications. J Popul Therapeutics Clin Pharmacol = J de la Therapeutique des Popul et de la Pharmacologie Clin. 2022;28(2):29–40.
- [28] Mondal P, Anweshan A, Purkait MK. Green synthesis and environmental application of iron-based nanomaterials and nanocomposite: a review. Chemosphere. 2020;259:127509.
- [29] Chockalingam S, Preetha S, Jeevitha M, Pratap L. Antibacterial Effects of Capparis decidua Fruit Mediated Selenium Nanoparticles. J Evol Med Dent Sci. 2020;9:2947–51.
- [30] Zakariya NA, Majeed S, Jusof WHW. Investigation of antioxidant and antibacterial activity of iron oxide nanoparticles (IONPS) synthesized from the aqueous extract of Penicillium spp. Sens Int. 2022;3:100164.
- [31] Zangeneh A, Zangeneh MM, Moradi R. Ethnomedicinal plantextract-assisted green synthesis of iron nanoparticles using Allium saralicum extract, and their antioxidant, cytotoxicity, antibacterial, antifungal and cutaneous wound-healing activities. Appl Organomet Chem. 2020;34(1):e5247.
- [32] Vitta Y, Figueroa M, Calderon M, Ciangherotti C. Synthesis of iron nanoparticles from aqueous extract of Eucalyptus robusta Sm and evaluation of antioxidant and antimicrobial activity. Mater Sci Energy Technol. 2020;3:97–103.
- [33] Shnoudeh AJ, Hamad I, Abdo RW, Qadumii L, Jaber AY, Surchi HS, et al. Synthesis, characterization, and applications of metal nanoparticles. In: Biomaterials and Bionanotechnology. MDPI: Academic Press; 2019. p. 527–612.
- [34] Gunti L, Dass RS, Kalagatur NK. Phytofabrication of selenium nanoparticles from Emblica officinalis fruit extract and exploring its biopotential applications: antioxidant, antimicrobial, and biocompatibility. Front Microbiology. 2019;10:931.
- [35] Adibian F, Ghaderi RS, Sabouri Z, Davoodi J, Kazemi M, Ghazvini K, et al. Green synthesis of selenium nanoparticles using *Rosmarinus officinalis* and investigated their antimicrobial activity. BioMetals. 2022;35:147–58.
- [36] Sarkar J, Dey P, Saha S, Acharya K. Mycosynthesis of selenium nanoparticles. Micro Nano Lett. 2011;6(8):599–602.
- [37] Safaei M, Mozaffari HR, Moradpoor H, Imani MM, Sharifi R, Golshah A. Optimization of green synthesis of selenium nanoparticles and evaluation of their antifungal activity against oral *Candida albicans* infection. Adv Mater Sci Eng. 2022;2022:1–8.
- [38] Al-Qaraleh SY, Al-Zereini WA, Oran SA, Al-Sarayreh AZ, Sa'ed M. Evaluation of the antioxidant activities of green synthesized

- selenium nanoparticles and their conjugated polyethylene glycol (PEG) form in vivo. Open Nano. 2022;8:100109.
- [39] Liu Y, Li F, Zhang L, Wu J, Wang Y, Yu H. Taurine alleviates lipopolysaccharide-induced liver injury by anti-inflammation and antioxidants in rats. Mol Med Rep. 2017;16(5):6512–7.
- [40] Filipović N, Ušjak D, Milenković MT, Zheng K, Liverani L, Boccaccini AR, et al. Comparative study of the antimicrobial activity of selenium nanoparticles with different surface chemistry and structure. Front Bioeng Biotechnol. 2021;8:624621.
- [41] Truong LB, Medina-Cruz D, Mostafavi E, Rabiee N. Selenium nanomaterials to combat antimicrobial resistance. Molecules. 2021;26(12):3611.
- [42] Velsankar K, RM AK, Preethi R, Muthulakshmi V, Sudhahar S. Green synthesis of CuO nanoparticles via Allium sativum extract and its characterizations on antimicrobial, antioxidant, antilarvicidal activities. J Environ Chem Eng. 2020;8(5):104123.
- [43] Prathna TC, Chandrasekaran N, Raichur AM, Mukherjee A. Biomimetic synthesis of silver nanoparticles by Citrus limon (Lemon) aqueous extract and theoretical prediction of particle size. Colloid Surf B: Bioint. 2011 Jan;82:152–9.
- [44] javed B, Nadhman A, Mashwani Z. Optimization, characterization and antimicrobial activity of silvernanoparticles against plant bacterial pathogens phyto-synthesized by Mentha longifolia. Mater ResExpress. 2020;7:085406.
- [45] Wang W, Tang Q, Yu T, Li X, Gao Y, Li J, et al. Surfactant-free preparation of Au@ resveratrol hollow nanoparticles with photothermal performance and antioxidant activity. ACS Appl Mater Interfaces. 2017;9:3376–87.
- [46] Bhakya S, Muthukrishnan S, Sukumaran M, Muthukumar M. Biogenic synthesis of silver nanoparticles and their antioxidant and antibacterial activity. Appl Nanosci. 2016;6:755–66.
- [47] Senthilkumar SR, Sivakumar T. Green tea (Camellia sinensis) mediated synthesis of zinc oxide (ZnO) nanoparticles and studies on their antimicrobial activities. Int J Pharm Pharm Sci. 2014;6(6):461–5.
- [48] Baliah NT, Muthulakshmi P, Sheeba PC, Priyatharsini SL. Green synthesis and characterization of nanocomposites. Int Res J Eng Technol. 2018;5(12):179–86.
- [49] Prasad KS, Patel H, Patel T, Patel K, Selvaraj K. Biosynthesis of Se nanoparticles and its effect on UV-induced DNA damage. Colloids Surf B: Biointerfaces. 2013:103:261–6.
- [50] Gangadoo S, Stanley D, Hughes RJ, Moore RJ, Chapman J. The synthesis and characterisation of highly stable and reproducible selenium nanoparticles. Inorg Nano-Metal Chem. 2017;47(11):1568–76.
- [51] Vahdati M, Tohidi Moghadam T. Synthesis and characterization of selenium nanoparticles-lysozyme nanohybrid system with synergistic antibacterial properties. Sci Rep. 2020;10(1):1–10.
- [52] Fesharaki PJ, Nazari P, Shakibaie M, Rezaie S, Banoee M, Abdollahi M, et al. Biosynthesis of selenium nanoparticles using Klebsiella pneumoniae and their recovery by a simple sterilization process. Braz | Microbiol. 2010;41:461–6.
- [53] Ramamurthy CH, Sampath KS, Arunkumar P, Kumar MS, Sujatha V, Premkumar K, et al. Green synthesis and characterization of selenium nanoparticles and its augmented cytotoxicity with doxorubicin on cancer cells. Bioprocess Biosyst Eng. 2013;36(8):1131–9.
- [54] Jagathesan G, Rajiv P. Biosynthesis and characterization of iron oxide nanoparticles using Eichhornia crassipes leaf extract and assessing their antibacterial activity. Biocatalysis Agric Biotechnol. 2018;13:90–4.

[55] Tartaj P, del Puerto Morales M, Veintemillas-Verdaguer S, González-Carreño T, Serna CJ. The preparation of magnetic nanoparticles for applications in biomedicine. J Phys D: Appl Phys. 2003;36(13):R182.

DE GRUYTER

- [56] Abdullah JAA, Eddine LS, Abderrhmane B, Alonso-González M, Guerrero A, Romero A. Green synthesis and characterization of iron oxide nanoparticles by pheonix dactylifera leaf extract and evaluation of their antioxidant activity. Sustain Chem Pharm. 2020;17:100280.
- [57] Kelly KL, Coronado E, Zhao LL, Schatz GC. The optical properties of metal anoparticles: The influence of size, shape and dielectric environment. J Phys Chem. 2003;107:668-77.
- [58] Anu K, Singaravelu G, Murugan K, Benelli G. Green-synthesis of selenium nanoparticles using garlic cloves (Allium sativum): biophysical characterization and cytotoxicity on vero cells. J Clust Sci. 2017:28:551-63.
- [59] Sree BS, Aparna Y, Babu TA, Krishna NV. Indium tin oxide nanocomposites-green synthesis, characterization, morphology and optical properties using Almond Gum. Lett Appl NanoBioScience. 2022;11(1):3134-41.
- [60] Prasad KS, Selvaraj K. Biogenic synthesis of selenium nanoparticles and their effect on As (III)-induced toxicity on human lymphocytes. Biol Trace Elem Res. 2014;157:275-83.
- [61] Batool F, Iqbal MS, Khan SUD, Khan J, Ahmed B, Qadir MI. Biologically synthesized iron nanoparticles (FeNPs) from Phoenix dactylifera have anti-bacterial activities. Sci Rep. 2021;11(1):22132.
- [62] Lakshminarayanan S, Shereen MF, Niraimathi KL, Brindha P, Arumugam A. One-pot green synthesis of iron oxide nanoparticles from Bauhinia tomentosa: Characterization and application towards synthesis of 1, 3 diolein. Sci Rep. 2021;11(1):1-13.
- [63] Alagesan V, Venugopal S. Green synthesis of selenium nanoparticle using leaves extract of withania somnifera and its biological applications and photocatalytic activities. Bionanoscience. 2019;9(1):105-16.
- [64] Nahari MH, Al Ali A, Asiri A, Mahnashi MH, Shaikh IA, Shettar AK, et al. Green synthesis and characterization of iron nanoparticles synthesized from aqueous leaf extract of vitex leucoxylon and its biomedical applications. Nanomaterials. 2022;12(14):2404.
- [65] Zimmerman MT, Bayse CA, Ramoutar RR, Brumaghim JL. Sulfur and selenium antioxidants: challenging radical scavenging mechanisms and developing structure-activity relationships based on metal binding. J Inorg Biochem. 2015;145:30-40.
- [66] Singh J, Kumar S, Dhaliwal A. Controlled release of amoxicillin and antioxidant potential of gold nanoparticles-xanthan gum/poly (Acrylic acid) biodegradable nanocomposite. J Drug Deliv Sci Technol. 2019;55:101384.
- [67] Vyas J, Rana S. Antioxidant activity and green synthesis of selenium nanoparticles using allium sativum extract. Int J Phytomedicine. 2017;9(4):634-41.
- [68] Kokila K, Elavarasan N, Sujatha V. Disopyros montana leaf extractmediated synthesis of selenium nanoparticles and their biological applications. N J Chem. 2017;41:7481-90. doi: 10.1039/c7nj01124e.
- Chavan RR, Bhinge SD, Bhutkar MA, Randive DS, Wadkar GH, Todkar SS, et al. Characterization, antioxidant, antimicrobial and cytotoxic activities of green synthesized silver and iron nanoparticles using alcoholic Blumea eriantha DC plant extract. Mater Today Com. 2020;24:101320.

- [70] Lin YL, Juan IM, Chen YL, Liang YC, Lin JK. Composition of polyphenols in fresh tea leaves and associations of their oxygenradical-absorbing capacity with antiproliferative actions in fibroblast cells. J Agric Food Chem. 1996;44:1387-94.
- Deshmukh AR, Gupta A, Kim BS. Ultrasound assisted green synthesis of silver and iron oxide nanoparticles using fenugreek seed extract and their enhanced antibacterial and antioxidant activities. BioMed Res Int. 2019:2019:51-94.
- [72] Hassan HU, Raja NI, Abasi F, Mehmood A, Qureshi R, Manzoor Z, et al. Comparative Study of Antimicrobial and Antioxidant Potential of Olea ferruginea Fruit Extract and Its Mediated Selenium Nanoparticles. Molecules. 2022;27(16):5194.
- [73] Chau TP, Brindhadevi K, Krishnan R, Alyousef MA, Almoallim HS, Whangchai N, et al. A novel synthesis, analysis and evaluation of Musa coccinea based zero valent iron nanoparticles for antimicrobial and antioxidant. Environ Res. 2022;209:112770.
- [74] Fardsadegh B, Jafarizadeh-Malmiri H. Aloe vera leaf extract mediated green synthesis of selenium nanoparticles and assessment of their in vitro antimicrobial activity against spoilage fungi and pathogenic bacteria strains. Green Process Synth. 2019;8(1):399-407.
- Nwamezie OUIF. Green synthesis of iron nanoparticles using [75] flower extract of Piliostigma thonningii and their antibacterial activity evaluation. Chem Int. 2018;4(1):60.
- [76] Tran PA, O'Brien-Simpson N, Reynolds EC, Pantarat N, Biswas DP, O'Connor AJ. Low cytotoxic trace element selenium nanoparticles and their differential antimicrobial properties against S. aureus and E. coli. Nanotechnology. 2015;27(4):045101.
- Gurunathan S, Han JW, Dayem AA, Eppakayala V, Kim JH. Oxidative [77] stress-mediated antibacterial activity of graphene oxide and reduced graphene oxide in Pseudomonas aeruginosa. Int J Nanomed. 2012;7:5901.
- [78] Nagy A, Harrison A, Sabbani S, Munson Jr RS, Dutta PK, Waldman WJ. Silver nanoparticles embedded in zeolite membranes: release of silver ions and mechanism of antibacterial action. Int J Nanomed. 2011;6:1833.
- Leung YH, Ng AM, Xu X, Shen Z, Gethings LA, Wong MT, et al. [79] Mechanisms of antibacterial activity of MgO: non-ROS mediated toxicity of MgO nanoparticles towards Escherichia coli. Small. 2014:10(6):1171-83.
- [80] Weir E, Lawlor A, Whelan A, Regan F. The use of nanoparticles in anti-microbial materials and their characterization. Analyst. 2008;133(7):835-45.
- Martínez-Esquivias F, Guzmán-Flores JM, Pérez-Larios A, González Silva N, Becerra-Ruiz JS. A review of the antimicrobial activity of selenium nanoparticles. J Nanosci Nanotechnol. 2021;21(11):5383-98.
- [82] Zhang H, Li Z, Dai C, Wang P, Fan S, Yu B, et al. Antibacterial properties and mechanism of selenium nanoparticles synthesized by Providencia sp. DCX. Environ Res. 2021;194:110630.
- Devatha CP, Jagadeesh K, Patil M. Effect of Green synthesized iron nanoparticles by Azardirachta Indica in different proportions on antibacterial activity. Environ Nanotechnol Monit Manag. 2018;9:85-94.